Optical model of the blood in large retinal vessels

Kurt R. Denninghoff
University of Alabama at Birmingham
Department of Emergency Medicine
JT N. 266, 619 South 19th Street
Birmingham, Alabama 35233-7013

Matthew H. Smith
University of Alabama in Huntsville
Department of Physics, OB-318
Huntsville, Alabama 35899

Abstract. Several optical techniques that investigate blood contained within the retinal vessels are available or under development. We present a mechanical model that simulates the optical properties of the eye, the retinal vessels, and the ocular fundus. A micropipette is chosen as the retinal vessel model, and a mechanical housing is constructed to simulate the eyeball. Spectralon is used to simulate the retinal layers. Filling the eye with fluid index matched to the glass pipette eliminates reflection and refraction effects from the pipette. An apparatus is constructed and used to set the oxygen, nitrogen, and carbon dioxide concentrations in whole human blood. These whole blood samples are pumped through the pipette at 34 μL/min. Measurements made in the model eye closely resemble measurements made in the human eye. This apparatus is useful for developing the science and testing the systems that optically investigate blood and blood flow in the large retinal vessels. © *2000 Society of Photo-Optical Instrumentation Engineers.* [S1083-3668(00)00404-4]

Keywords: retinal vessels; retinal blood flow; oximetry; noninvasive monitoring; tissue phantoms.

1 Introduction

Several optical techniques that investigate the arteries and veins of the retina are either commercially available or are under development. These techniques include retinal Doppler flowmetry,[1] speckle flowmetry,[2] spectroscopic blood oximetry,[3–7] and dynamic measurements of vessel pulsations.[8] The optical accessibility of the retina facilitates these techniques, however getting light into and out of the eye presents several interesting problems. Some of these challenges include pigment variability in the retina, lens cataracts, irregular vessel shape, vessel proximity, and large underlying choroidal vessels.

We present an inexpensive mechanical model that simulates the optical geometry of the eye, the blood flowing in a retinal vessel, and the diffuse reflectance properties of the ocular fundus. We also describe an apparatus used to set the hemoglobin concentration and oxygen saturation of a blood sample without affecting the geometry of the red blood cells (and thus the scattering properties of the blood). The model does not include such confounding effects as the polarization influences of the cornea and nerve fiber layer, the optical properties of the vessel wall, the irregular choroidal blood vessels beneath the retinal pigmented epithelium, and the scattering properties of the crystalline lens or vitreous. Removing these difficulties allows us to directly explore the absorption and scattering properties of the blood within a retinal vessel, which is a critical first step in the development of a measurement technique. We review some of the scientific progress we have made in the field of retinal vessel oximetry through the use of this model.

2 Materials and Methods

A 5 μL micropipette (Fisherbrand disposable micropipettes, Cat. 21-164-2B, Fisher Scientific) was chosen as the retinal vessel model. The 10 cm length facilitated mounting and grasping, and the 268 μm inner diameter is slightly larger than the largest retinal veins (212 μm) and arteries (150 μm).[8] To more closely approximate these dimensions, the pipettes were gently pulled on a lathe while softened with a Bunsen burner. The resulting tapered pipettes had inner diameters ranging from 110 to 268 μm.

These micropipettes are manufactured from a borosilicate glass with a nominal refractive index of $n_d = 1.4712$. As a result, the pipette acts as a powerful cylindrical lens, and this optical power must be removed in order to be useful as a model. Standard type A immersion oil (Cargille Laboratories, Cedar Grove, NJ) was purchased as an inexpensive replacement for more expensive index matching fluids. The index of type A oil is $n_d = 1.5150$, which is slightly too high to provide a good index match to the pipettes. We titrated the type A oil with mineral spirits ($n_d = 1.438$ as measured by an Abbe refractometer) and index matched the pipette such that it was completely invisible to visual inspection when immersed in the fluid.

We used a slab of Spectralon (Labsphere, Inc.) adhered to an aluminum plate as a tissue phantom simulating the retinal layers. Spectralon is a diffusely reflective, spectrally neutral material typically used in integrating spheres. By modifying the thickness of the Spectralon slab, we were able to control the size of the diffusion-enlarged point spread function on the simulated retina. We use a 4-mm-thick slab of Spectralon that results in a diffusion enlarged point spread function (PSF) that is ~40 μm full width at half maximum. This compares well

Address all correspondence to Kurt R. Denninghoff, M.D. Tel: 205-975-7458; Fax: 205-975-4662; E-mail: kdenning@uabmc.edu
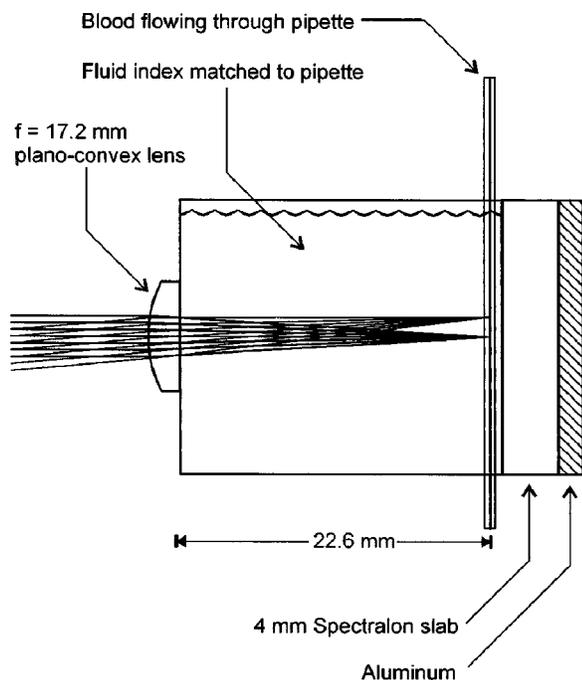
Blood flowing through pipette

Fluid index matched to pipette

f = 17.2 mm
plano-convex lens

22.6 mm

4 mm Spectralon slab

Aluminum

Fig. 1 Schematic of the model eye and blood vessel. A pipette filled with whole blood is immersed in index matched fluid and positioned in front of a piece of Spectralon. A plano-convex lens simulates the refractive power of the cornea and lens. Incoming rays from infinitely distant objects that are on axis and 5° off axis are shown.

with estimated retinal PSFs for visible wavelengths reported in the literature.[9] Using thicker slabs of Spectralon results in larger PSFs. Alternately, other researchers have suggested latex microspheres suspended in epoxy as a useful phantom to simulate the diffuse reflectance properties of tissues.[10]

We constructed a mechanical housing which simulates the eyeball (see Figure 1). The housing is filled with the index matching fluid. A plano-convex lens (Royln Optics, 10.0025) adhered to the housing with MIL-Bond is used to simulate the cornea. This lens has a focal length of 17.2 mm in air, but closely approximates the 23 mm focal length of the average human eye when the planar side of the lens is immersed in the index matched fluid. The entrance pupil diameter was set to 6 mm. The center of the pipette is located 22.6 mm behind the planar surface of the lens, and the Spectralon slab is positioned directly behind the pipette. An infinitely distant object that subtends 1° will form a 294 μm image on the retina of the model eye. This corresponds closely to the typical magnification (297 μm/°) of the normal human eye.[11] The model eye was constructed such that the pipettes could be positioned in various locations both on axis and off axis since the major vessels of the human eye are approximately 15° off axis. Bead blasting and black anodizing the inside of the mechanical housing prevents multiple reflections within the eye from exiting the pupil.

To simulate blood flow through the retinal vessel, a syringe pump (Harvard Apparatus, Model 55-1111) was used to pump whole human blood through a short length of tubing, and through the pipette. The pump was set to deliver blood at a typical value of retinal blood flow (34 μL/min).[12] A catch

basin collected the blood after it passed through the eye and was disposed of via approved methods.

Preparation of blood samples was carefully conducted to assure that a single variable was being modified throughout a given test. Whole human blood (500 cm^3) was drawn from a healthy donor according to an Internal Review Board approved protocol. The blood was anticoagulated (citrated dextrose) to prevent clotting during the measurement. The anticoagulant is not expected to affect the scattering measurement since it does not alter the red blood cell size or shape, and its small volume fraction will not significantly alter either the refractive indices of the components or their relative concentrations. The whole blood was immediately packed in ice and samples were drawn and prepared as needed. A sample of blood was centrifuged for approximately 5 min to separate the plasma from the cellular component of the blood. The packed blood cells and plasma were mixed volumetrically to make different concentrations of blood cells in plasma. The use of the patient's own plasma to dilute the blood minimizes changes in the size and shape of the red blood cells and possible color changes which may occur when isotonic salt solutions are used to dilute the blood.

A three-gas mixer was used to individually set the oxygen, nitrogen, and carbon dioxide concentrations of a combined gas. The total flow rate for the gas mixture was set at 3 L/min. The CO_2 flow was adjusted (~0.1 L/min.) to ensure the partial pressure of CO_2 in the blood was maintained at 35–45 mmHg, as measured by a blood gas machine (Corning 280 pH/Blood Gas Analyzer). The ratio between N_2 and O_2 flow rates was varied in order to set the oxygen saturation of the blood sample. This gas mixture was bubbled through a warm water bath saturating the gas with water vapor and warming it to body temperature. The warmed, humidified gas mixture was passed over the blood sample in a counter current exchange system as the blood was pumped through a closed circuit. A subsection of the blood circuit tubing was passed through a warm water bath (39°C) to keep it at body temperature during the oxygenation procedure. The blood was pumped through the system at a rate of 1000 mL/h. This system is illustrated in Figure 2. The blood was allowed to flow through the circuit for as long as is required to obtain the desired oxyhemoglobin saturation level, generally about 15 min. We used a CO-Oximeter (Corning 2500 CO-Oximeter) to measure the oxygen saturation and hemoglobin concentration of the prepared blood samples.

3 Results

Our primary purpose for developing this model was to test a scanning laser retinal vessel oximeter that we are developing.[4–6] The eye oximeter (EOX) shines low-power lasers into a subject's eye, and scans the beams across the retinal vasculature. The light that is scattered back out of the eye is collected and analyzed. Performing this measurement at multiple wavelengths allows spectroscopic determination of the oxygen saturation of blood contained within the arteries and veins of the retina. In Figure 3, we compare an EOX scan acquired from a human eye to a scan acquired from the model. These scans are one-dimensional spatial profiles of the collected intensity as a 629 nm beam is scanned perpendicularly across the vessel. In both cases, the vessel was illumi-
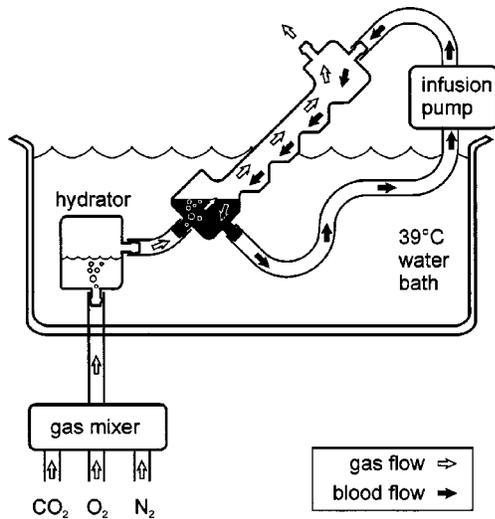
Fig. 2 Schematic of the apparatus for setting the oxygen saturation of whole blood. The apparatus allows the CO_2, O_2, and N_2 gas levels to be set while keeping the blood hydrated and at body temperature.

Fig. 4 Example of data acquired in the model eye. This graph is the result of the eye oximeter calibration experiment described in Ref. 13. Each data point represents a blood sample with different oxygen saturation and hemoglobin concentration. The error bars indicate the standard deviation of measurements made at different vessel diameters ranging from 110 to 268 μm.

nated with vertically polarized light and a horizontal polarizer in front of the detector attenuated the specular reflection that occurs at the refractive index discontinuity between the blood and the pipette (model eye) or the vessel wall (human eye). The similarity between the scans is obvious. The primary difference between the scans is that those acquired from the model eye have uniform intensity in regions lateral to the vessel, while human scans can be quite irregular in regions lateral to the vessel due to underlying choroidal vessels and variations in retinal pigmentation.

In a recent set of experiments, we used this model eye apparatus to calibrate a four-wavelength (629, 678, 821, and 899 nm) version of the EOX. We generated an array of blood samples with oxygen saturation values ranging from 6 to 87% O_2 Sat and hemoglobin concentrations ranging from 5.0 to 27.2 g/dL, and we used a variety of vessels with diameters ranging from 110 to 268 μm. A total of 187 different combinations were generated. This large array of known samples was used to determine a wavelength dependance of the red blood cell scattering. This allowed accurate calculation of oxygen saturation that was independent of hematocrit and

vessel diameter across normal ranges. The details of this experiment are reported elsewhere,[13,14] however we show the results of this calibration experiment in Figure 4.

In another experiment, we tested a second-generation EOX that was a modified confocal scanning laser ophthalmoscope capable of interlacing multiple lasers (488, 635, 670, and 830 nm) into a single video frame.[15] Measurements in the model eye exposed our lack of understanding of the light paths that comprised our measurement. We precisely knew the thickness of the pipette and the hemoglobin concentration of the sample, however fitting spectra to our measured vessel transmittances resulted in a *calculated* thickness-concentration product that was only 22% of the known value. These measurements led us to develop a theory demonstrating that backscattered light from red blood cells creates the appearance of a reduced path length through retinal vessels. The theory also explains the dependence of oximeter calibration due to fundus reflectivity that has been reported by other investigators.[16] We have described the details of this experiment elsewhere.[17]

4 Discussion and Conclusions

Using the model eye and blood preparation system described in this paper, we were able to develop an increased understanding of retinal vessel oximetry. This model should be useful for testing any systems that use light to study the blood and blood flow in retinal vessels. Such systems include fluorescent dye photography, laser speckle and Doppler flow experiments, and spectroscopic studies of blood constituents.

In this model we did not attempt to model the coloration of the retina (pigment epithelium), the choroidal circulation, scattering from the lens and vitreous, and the vessel wall. These interactions make the eye a complex environment, and we used this model in an attempt to decrease the number of these variables. As retinal vessel measurement techniques continue to mature, however, more complex models may be desired for further hypothesis testing. An extension of this work will be the creation of phantoms that model both the
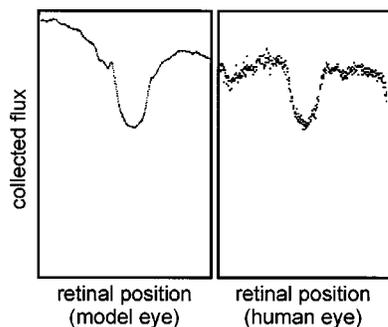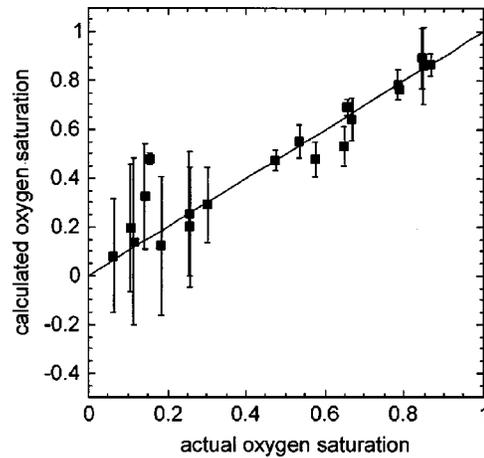

Fig. 3 Comparison of one-dimensional retinal vessel intensity profiles. The scan on the left was acquired in the model eye and the scan on the right was acquired in a human eye. Note the decreased noise in the model eye scan that is due to the high reflectivity of Spectralon.

scattering properties and the coloration of the human ocular fundus. The Spectralon background used in our experiments was 100% reflective, but we are now investigating 2% and 10% reflectance Spectralon backgrounds that more closely model the reflectance of typical retinal backgrounds. Alternately, human retinal tissue samples embedded in epoxy might prove to be the ultimate model for this system. Another improvement that should be made to the mode is the inclusion of an adjustable pupil diameter. Finally, the inclusion of impurities in the index matched fluid of the model eye might allow the scattering effects of the lens and vitreous to be modeled.

The primary weakness of our model is the lack of the vessel wall, which may have reflective, scattering, and possibly absorption properties that are not negligible. Simulating the vessel wall of a 120 μm vessel proves to be quite challenging, and we currently do not have a viable plan for creating this model.

A good *in vitro* model is imperative in the development of noninvasive techniques for measuring physiologic parameters. This is particularly true in the retina because actual values of the parameters being measured often cannot be measured directly for comparison. The inexpensive model described here has proven invaluable for advancing our understanding of retinal vessel oximetry.

Acknowledgments

References

1. A. Harris, L. Kagemann, and G. A. Cioffi, ''Assessment of human ocular hemodynamics,'' *Surv. Ophthalmol.* **42**(6), 509–533 (1998).
2. Y. Aizu and T. Asakura, ''Coherent optical techniques for diagnosis of retinal blood flow,'' *J. Biomed. Opt.* **4**(1), 61–75 (1999).
3. D. Schweitzer, M. Hammer, and M. Scibor, ''Imaging spectrometry in ophthalmology—principle and applications in microcirculation and in investigation of pigments,'' *Ophthalmic Res.* **28** Suppl. 2, 37–44 (1996).
4. J. M. Beach, K. J. Schwenzer, S. Srinivas, D. Kim, and J. S. Tiedeman, ''Oximetry of retinal vessels by dual-wavelength imaging: Calibration and influence of pigmentation,'' *J. Appl. Physiol.* **86**(2), 748–758 (1999).
5. K. R. Denninghoff, M. H. Smith, R. A. Chipman, L. W. Hillman, P. M. Jester, C. E. Hughes, F. Kuhn, and L. W. Rue, ''Retinal large vessel oxygen saturations correlate with early blood loss and hypoxia in anesthetized swine,'' *J. Trauma: Inj., Infect., Crit. Care* **43**(1), 29–34 (1997).
6. M. H. Smith, K. R. Denninghoff, L. W. Hillman, and R. A. Chipman, ''Oxygen saturation measurements of blood in retinal vessels during blood loss,'' *J. Biomed. Opt.* **3**(3), 296–303 (1998).
7. K. R. Denninghoff, M. H. Smith, L. W. Hillman, D. Redden, and L. W. Rue, ''Retinal venous oxygen saturation correlates with blood volume,'' *Acad. Emerg. Med.* **5**(6), 577–582 (1998).
8. H. C. Chen, V. Patel, J. Wiek, S. M. Rassam, and E. M. Kohner, ''Vessel diameter changes during the cardiac cycle,'' *Eye* **8**, 97–103 (1994).
9. J. Hodgkinson, P. B. Greer, and A. C. Molteno, ''Point-spread function for light scattered in the human ocular fundus,'' *J. Opt. Soc. Am. A* **11**(2), 479–486 (1994).
10. S. T. Flock, B. C. Wilson, and M. S. Patterson, ''Total attenuation coefficients and scattering phase functions of tissues and phantom materials at 633 nm,'' *Med. Phys.* **14**(5), 835–841 (1987).
11. D. Sliney and M. Wolbarsht, *Safety with Lasers and Other Optical Sources*, Chap. 3, Plenum, New York (1980).
12. T. F. Gilbert, T. Hiroshi, D. M. Deupree, D. G. Goger, J. Sebag, and J. J. Weiter, ''Blood flow in the normal human retina,'' *Invest. Ophthalmol. Visual Sci.* **30**, 58–65 (1989).
13. J. D. Drewes, M. H. Smith, D. R. Denninghoff, and L. W. Hillman, ''An instrument for the measurement of retinal vessel oxygen saturation,'' in *Optical Diagnostics of Biological Fluids IV*, Alexander V. Priezzhev, M. V. Lomonosov, Toshimitsu Asakura, Eds., *Proc. SPIE* **3591**, 114–120 (1999).
14. J. Drewes, ''Four wavelength retinal vessel oximetry,'' PhD Dissertation, University of Alabama in Huntsville, Huntsville, Ala., 1999.
15. A. Lompado, ''A confocal scanning laser ophthalmoscope for retinal vessel oximetry,'' PhD Dissertation, University of Alabama in Huntsville, Huntsville, Ala., 1999.
16. J. M. Beach, K. J. Schwenzer, S. Srinivas, and J. S. Tiedeman, ''Oximetry of retinal vessels by dual-wavelength imaging: Calibration and influence of pigmentation,'' *J. Appl. Physiol.* **86**, 748–758 (1999).
17. M. H. Smith, K. R. Denninghoff, A. Lompado, and L. W. Hillman, ''Effect of multiple light paths on retinal vessel oximetry,'' *Appl. Opt.* **39**(7), 1183–1193 (2000).